Journal of Luminescence 130 (2010) 669–673

Contents lists available at ScienceDirect

Journal of Luminescence

journal homepage: www.elsevier.com/locate/jlumin

Silicon nanocrystal synthesis by implantation of natural Si isotopes

D. Barba [a,*], D. Koshel [a], F. Martin [a], G.G. Ross [a], M. Chicoine [b], F. Schiettekatte [b], M. Yedji [c], J. Demarche [c], G. Terwagne [c]

[a] INRS-Centre Énergie Matériaux Télécommunications, Varennes, Québec, Canada J3X 1S2
[b] Département de Physique, Université de Montréal, Montréal, Québec, Canada H3T 1J4
[c] LARN, Centre de Recherche en Physique de la Matière et du Rayonnement, FUNDP, B-5000 Namur, Belgium

ARTICLE INFO

Article history:
Received 13 July 2009
Received in revised form
28 October 2009
Accepted 5 November 2009
Available online 12 November 2009

Keywords:
Silicon nanocrystals
Isotopic effect
Raman spectroscopy

ABSTRACT

Implantations of pure $^{28}Si^+$, $^{29}Si^+$, and $^{30}Si^+$ into SiO_2 can provide significant insight into the formation of silicon nanocrystals (Si-nc) and their light emission properties. Si-nc produced with different fractions of the heavier Si isotopes have been characterized by Raman and photoluminescence spectroscopy. Weak Stokes shifts of the Si-nc phonon peaks indicate that both the implanted Si and the native Si from the SiO_2 substrate contribute to Si-nc nucleation. The Raman measurements also indicate that the Si isotopic composition of the Si-nc is similar to the Si isotopic fraction of the implanted SiO_2. The Si-nc photoluminescence (PL) spectra are shifted towards the blue with increasing Si isotope mass, an indication that the increase of the Si-nc effective mass enhances the excitonic bandgap. Measurements from samples implanted with heavy isotopes at high Si excess concentrations indicate that the Si-nc isotope fraction evolves with annealing time such that the heaviest Si isotope are more concentrated in the vicinity of the $Si-nc/SiO_2$ interface, which can modify the energy states involved in the radiative transitions associated with Si-nc.

1. Introduction

The formation of Si nanocrystals (Si-nc) results from the clustering of Si atoms in excess produced by silicon implantation into silica or chemical deposition of substoichiometric SiO_x layers, under thermal activation [1,2]. The poor mobility of Si means that the Si-nc nucleation occurs from the clustering of Si atoms confined within a small volume of the oxide layer [3]. To better understand the Si-nc growing mechanism and to model the optical properties of emitting layers [4], it is important to clearly identify the origin of the silicon involved in the Si-nc nucleation, especially in samples prepared by ion implantation, where the SiO_2 target molecules can be dissociated by the implanted Si ions. Although the Si atoms nominally contained within the SiO_2 target can contribute to the formation of Si-nc, this is not sufficient since the implantation of Ar or Ne ions into SiO_2 at equivalent ion-fluences does not lead to the production of Si-nc [5].

In order to distinguish between the Si atoms coming from the ion implantation and the dissociated SiO_2 molecules, $^{29}Si^+$ and $^{30}Si^+$ have been implanted into natural fused silica substrates, where the ^{28}Si contents strongly dominates (^{28}Si: 92.2 at%, ^{29}Si: 4.7 at%, ^{30}Si: 3.1 at%). A standard process is then used to produce Si-nc from the implanted Si isotopes and to compare their Raman and PL emissions to those of Si-nc systems obtained from implantation of pure $^{28}Si^+$ [2,4]. These studies have allowed us to characterize the effect of Si isotopic concentration on both the phonon energy and the PL-emission of Si-nc, for annealing times varying between 15 and 120 min. The changes observed in the PL peak energy indicate significant variations of the Si-nc excitonic bandgap. A large concentration of ^{28}Si coming from the SiO_2 layer is detected in the Raman signature of Si-nc, whose evolution as a function of the annealing duration suggests slight variations of the Si isotope diffusivity.

2. Experiments

$^{28}Si^+$, $^{29}Si^+$ and $^{30}Si^+$ ions with energies between 50 and 150 keV were implanted at room temperature into fused silica with ions fluences varying between 1 and 2×10^{17} Si^+ cm^{-2}. According to SRIM simulations [6], the maximum concentrations of Si excess generated by these implantations are: 30% and 40% for ^{28}Si, 43% for ^{29}Si, and 28% and 43% for ^{30}Si. The post-implantation annealing was performed at 1100 °C under an atmosphere of N_2. The samples were then passivated at 500 °C in a N_2/H_2 (95:5) forming gas. In order to check the high isotopic purity of the implanted ions, implantations of $^{30}Si^+$ were performed with an

* Corresponding author.
E-mail address: barba@emt.inrs.ca (D. Barba).

0022-2313/$ - see front matter © 2009 Elsevier B.V. All rights reserved.
doi:10.1016/j.jlumin.2009.11.014

IMC-200 implanter ($m/\Delta m = 100$) and a Tandetron accelerator, using two different ion sources (Freeman SiF_4 gas and sputtering of ^{30}Si powder). After annealing and passivation, the Raman and PL spectra of these two sets of samples are identical.

Micro-Raman backscatter measurements were carried out at room temperature using a confocal Invia Renishaw RM 3000 spectrometer, equipped with a digital camera and a 50× objective lens of 0.75 NA. A 514.5 nm, 2.6 mW Ar laser line was used for the Raman excitation. The PL measurements were recorded using an USB2000 Ocean Optics spectrograph and a 1 mW 405 nm laser diode.

3. Results and discussion

Fig. 1 shows the Stokes shift variations of the Si-nc optical phonon associated with the vibrations of Si–Si bonds for the different implanted Si isotopes [7,8]. Comparison of the data obtained after 1 h thermal annealing indicates that the Si-nc phonon energy decreases continuously for increasing Si isotope mass. We observe Si-nc phonon peaks at 517.8 and 514.2 cm^{-1} (Fig. 1a) in the samples containing a concentration of 30% ^{28}Si and 28% ^{30}Si in excess, respectively. In samples implanted with 43% Si excess (Fig. 1b), Si-nc phonon peaks are observed at 518.8 cm^{-1} for ^{28}Si, 514.9 cm^{-1} for ^{29}Si and 512.1 cm^{-1} for ^{30}Si. Note that the phonon wavenumber of Si-nc produced from implanted ^{28}Si is smaller for maximum Si excess of 30% than 40%, as expected for the Raman signature of smaller Si-nc [7,8]. The fact that a lower concentration of Si in excess produces smaller Si-nc is supported by the PL-spectra blueshift shown in Fig. 2. Since all the studied samples were prepared using the same thermal treatment, and since the lattice parameter of Si at room temperature does not change significantly after isotopic substitution [9], we can assume that the average size of the produced Si-nc is equivalent in materials containing a similar concentration of Si in excess. The changes in phonon energy are associated with isotopic effects on Si–Si bond vibrations. However, we note that the Si-nc phonon wavenumbers of samples implanted with ^{29}Si and ^{30}Si isotopes are significantly larger than would be expected from the $M^{-1/2}$ dependence of the phonon frequency [10], calculated from

$$\omega(M_2) \simeq \omega(M_1)\sqrt{M_1/M_2} \quad (1)$$

where $M_1 = 28$ and M_2 is the Si isotope mass. Applied to Si nanocrystallites with similar dimensions, this relation predicts wavenumbers of pure ^{29}Si–^{29}Si and ^{30}Si–^{30}Si bond vibrations near 510 and 501 cm^{-1}, instead of the measured values of 514.9 and 512.1 cm^{-1} from samples with 43% Si excess. Such a discrepancy clearly shows that the formed Si-nc are grown from a mixture of the implanted Si isotopes and the ^{28}Si nominally present within the fused silica substrate, the latter being displaced during the collision cascade produced by the impinging ions. Using a virtual crystal approximation [11], we can estimate the relative

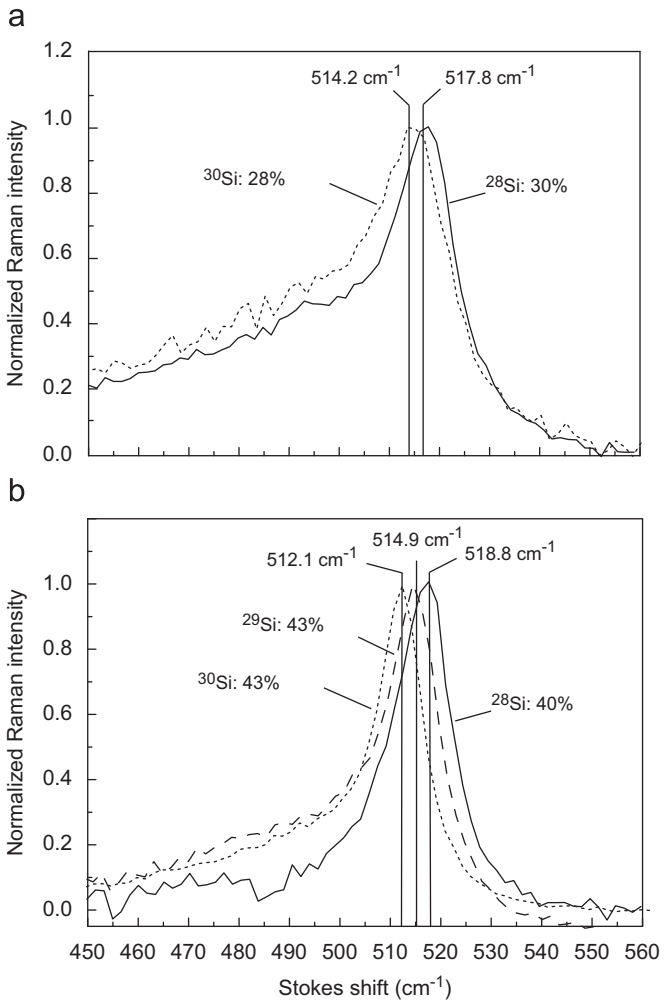

Fig. 1. Isotopic effect on the Si-nc optical phonon.

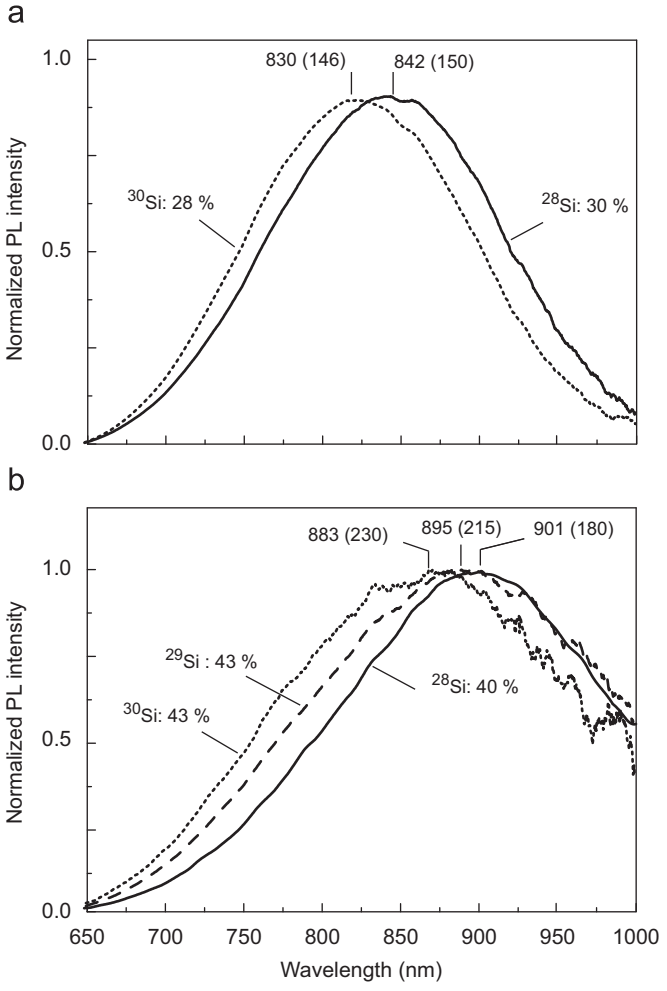

Fig. 2. Blueshifted PL-emission of Si-nc induced by isotopic effect with the measured wavelength position and bandwidth (brackets) of the PL peak.

concentration (x) of the implanted Si isotope effectively participating in the Si-nc nucleation from the observed Raman shifts. By neglecting the Si isotopic composition of natural SiO_2, whose contribution is smaller than the accuracy of our estimate, the calculations are performed using the following relation:

$$x = (\omega_0 - \omega_{meas})/(\omega_0 - \omega_{calc} - \delta\omega) \quad (2)$$

Table 1
Parameters used to calculate the Si isotopic composition of Si-nc (x).

Isotope	Si excess (%)	ω_0 (cm^{-1})	ω_{meas} (cm^{-1})	ω_{calc} (cm^{-1})	$\delta\omega$ (cm^{-1})	x (%)
^{29}Si	43	518.8	514.9	509.8	1.0	48
^{30}Si	28	517.8	514.2	500.2	0.5	21
^{30}Si	43	518.8	512.1	501.2	1.0	40

where ω_0 is the measured phonon wavenumber of Si-nc produced from implanted ^{28}Si, ω_{meas} is the measured phonon wavenumber of Si-nc produced from implanted Si isotopes, ω_{calc} is the expected value determined from Eq. (1), and $\delta\omega$ is a correction term associated with anharmonicity and isotope mass disorder [10,11]. As summarized in Table 1, the isotopic concentration of Si within the Si-nc is similar to the excess of implanted Si isotope introduced within SiO_2, namely: $48 \pm 6\%$ of ^{29}Si for the sample containing 43% of ^{29}Si in excess, and $40 \pm 3\%$ and $21 \pm 7\%$ of ^{30}Si for the samples containing 43% and 28% ^{30}Si in excess, respectively. Such a result indicates that during an annealing at 1100 °C for 1 h, the Si atoms coming from fused silica and the implanted Si participate equally to the Si-nc nucleation process.

Fig. 2 shows the isotopic effect on the Si-nc photoluminescence spectra for implanted Si in excess of 28% (Fig. 2a) and 43% (Fig. 2b). All spectral intensities have been normalized with

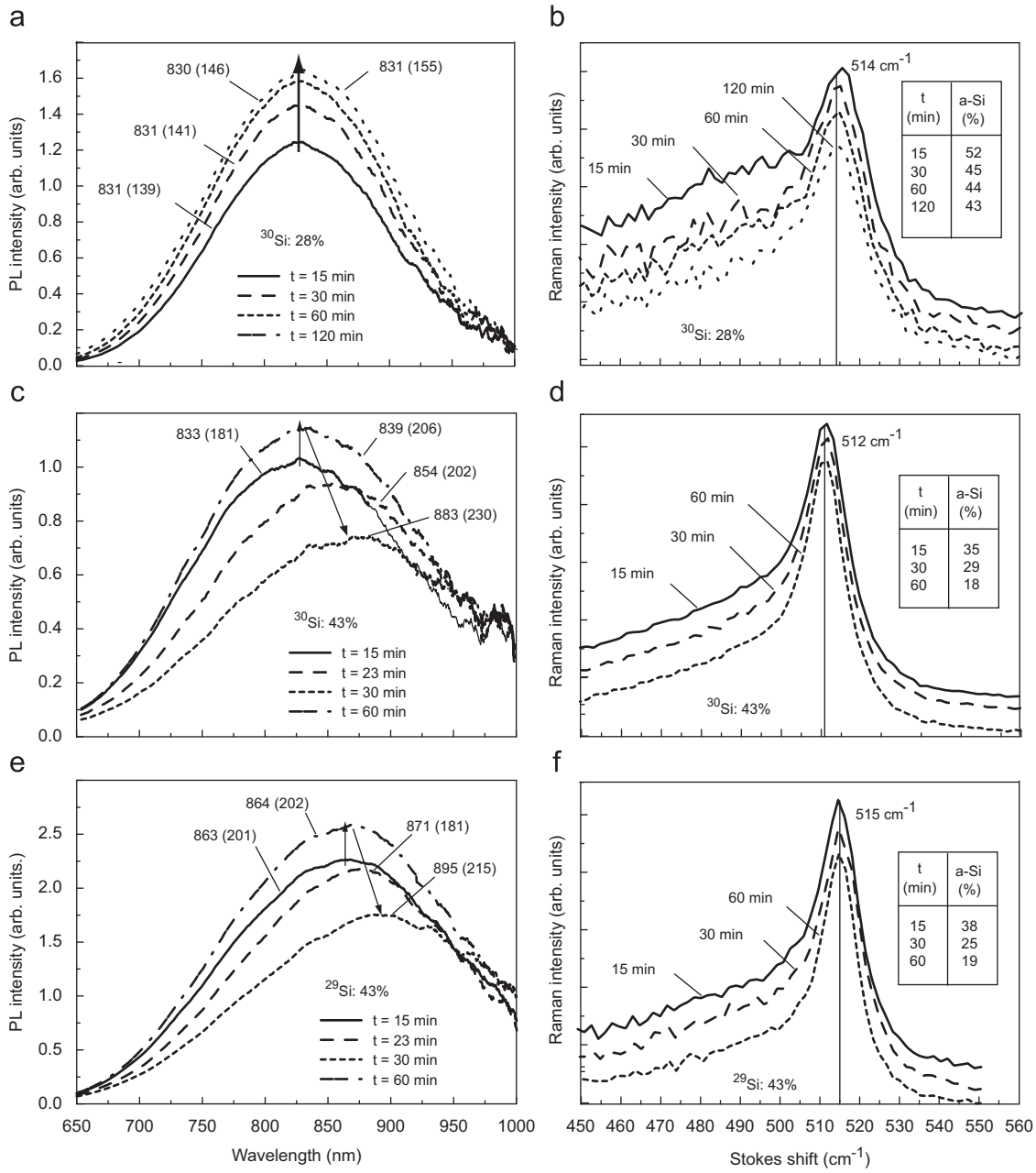

Fig. 3. Effect of the annealing time at 1100 °C on the PL-spectra (left) and the normalized Raman signature (right) of samples containing 28% of ^{30}Si in excess (a and b), 43% of ^{30}Si in excess (c and d), and 43% of ^{29}Si in excess (e and f). Table insets: relative concentrations of amorphous Si clusters evaluated from Ref. [13].

Table 2
Isotopic effect on the PL-peak position and energy of Si-nc.

Isotope	Si excess (%)	λ_{max} (nm)	Blueshift (nm)	E (meV)	ΔE (meV)
^{28}Si	30	842	–	1473	–
^{28}Si	40	901	–	1376	–
^{29}Si	43	895	6	1385	9
^{30}Si	28	830	12	1494	21
^{30}Si	43	883	18	1404	19

respect to the PL-emission of samples implanted with $^{28}Si^{+}$. We observe that the Si ion mass affects both maximum wavelength and spectral bandwidth of PL-emission, whose measured values are directly reported in the figure. As shown by Fig. 3c and e, discussed in the next paragraph, such a tendency is not affected by the duration of thermal annealing. As indicated in Table 2, the measured PL-peak is increasingly shifted towards the blue for the heavier isotopes. The corresponding PL-emission energy and energy variations as a function of implanted isotopes are given in meV in the two last columns of Table 2 for ease of comparison with previous works. Such variations of the PL-emission are greater than the expected weak dependence on isotopic mass at room temperature [10], and significantly stronger than those observed at low temperature in isotopically enriched Si crystals [12]. By studying the phonon-assisted transitions between 1050 and 1170 nm, Tsoi et al. have reported a maximum increase of the PL-emission energy of only 2 meV for materials containing more than 91% and 88% of ^{29}Si and ^{30}Si, respectively, attributed to an excitonic bandgap renormalization induced by electron–phonon coupling. This cannot account for the spectral changes observed in our measurements. However the electron–phonon coupling efficiency could be affected by the isotopic content, increasing the contribution of small Si-nc and thus shifting the spectrum towards the blue [13]. Also, it is possible that the isotopic substitution of ^{28}Si within nanocrystallites affects the nature of the Si-nc radiative states. This last effect may result from the creation of new electron energy states at the $Si-nc/SiO_2$ interface, related to changes in the Si-nc growing mechanism in the presence of a different Si isotope composition.

The effect of the annealing time on both the PL and the Raman spectra of samples implanted with ^{30}Si and ^{29}Si are presented in Fig. 3. Two distinct growing phases of Si-nc are observed for ^{30}Si excess concentrations of 28% and 43%, respectively. In Fig. 3a, the PL intensity of samples containing 28% of ^{30}Si in excess increases up to saturation at longer annealing times. No spectral shift is observed in the Si-nc PL-emission, as expected for systems containing Si-nc of small and uniform dimensions [2]. In parallel, for longer annealing times (Fig. 3b), the Raman spectra of samples with 28% of ^{30}Si excess show a significant decrease of the Si amorphous peak around 480 cm^{-1} with respect to the Si-nc phonon peak intensity. This spectral change is associated with the crystallization of amorphous Si (a-Si) clusters, whose relative concentrations, evaluated from Ref. [14], are directly reported in the figure. No energy shift is observed for the Si-nc phonon peak indicating that the Si isotopic concentration within the Si-nc is not effected by the annealing time. This suggests that the number of Si atoms contained within the nanocrystallites remains unchanged for annealing times greater than 15 min. The enhanced PL-emission of samples annealed for longer times (Fig. 3a) is associated with an increase of the emitter density, which could be due to a modification of the $Si-nc/SiO_2$ interface structure promoting radiative transitions [15]. In Fig. 3c, the PL intensity of samples with 43% ^{30}Si excess increases with annealing time up to 23 min. For greater annealing times, the PL-emission decreases and is shifted towards the red. The PL spectral shift (arrows) for annealing times longer than 23 min can be explained by the formation of larger Si-nc from the clustering of small Si-nc produced at the beginning of the thermal annealing [16]. In Fig. 3d, the Si-nc phonon peak narrows and the contribution of a-Si phonon to the Raman spectra decreases for increasing annealing times. The narrowing of the Si-nc peak reveals the presence of a higher density of Si–Si bonds within the medium, in agreement with the formation of larger nanocrystals within systems containing a high content of Si excess [2]. A similar evolution of the PL and Raman spectra (Fig. 3e and f) is observed for samples containing 43% of ^{29}Si in excess. However, no significant change of the phonon peak is observed for long annealing times, in spite of the expected increase of the Si-nc phonon wavenumber with the nanocrystallite dimensions [7]. These Raman shifts could be masked by the slower thermal diffusivity of ^{30}Si and ^{29}Si, compared to that of ^{28}Si, an effect that is weakened in systems containing a lower concentration of implanted Si where the largest average distance between Si atoms in excess favours their dilution within the oxide [2]. In such a scenario, the increase of the Si-nc phonon energy resulting from the coalescence of small Si-nc in larger nanocrystallites would be compensated by a more belated clustering of Si isotopes. This implies that the heaviest Si isotope are more concentrated in the vicinity of $Si-nc/SiO_2$ interface, where any modification of the energy states involved in the radiative transition can affect the PL-spectra of Si-nc.

4. Conclusion

We have demonstrated that both the implanted Si ions and the native Si atoms from the SiO_2 substrate contribute to the formation of Si-nc. The Si-nc isotopic fraction (after 1 h annealing) is similar to the Si composition of the implanted samples (before annealing), an indication that the Si-nc nucleation during thermal annealing does not differentiate between the implanted Si and the native Si from the SiO_2 substrate. We have shown that an increase of the Si isotope mass reduces both the Si–Si bond vibration energy in Si-nc and the wavelength of their PL-emission. The PL-spectra blueshift induced by isotopic substitution is associated with an increase of the excitonic bandgap of Si-nc resulting from changes of the Si-nc radiative states or/and enhanced photoemission from the smaller Si-nc. Raman measurements indicate that the heavier Si isotopes are more concentrated in the vicinity of $Si-nc/SiO_2$ interface, which can modify the energy states involved in the radiative transition observed in the PL-spectra of Si-nc.

Acknowledgements

This work was supported by the ST-4/05.804 Québec–Wallonie–Bruxelles collaboration, the Natural Science and Engineering Research Council of Canada, and Plasmionique Inc.

References

[1] F. Iacona, C. Bongiorno, C. Spinella, S. Boninelli, F. Priolo, J. Appl. Phys. 95 (7) (2004) 3723.
[2] Y.Q. Wang, R. Smirani, G.G. Ross, Nanotechnology 15 (2004) 1554.
[3] O. Jaoul, F. Béjina, F. Elie, F. Abel, Phys. Rev. Lett. 74 (11) (1995) 2038.
[4] D. Barba, C. Dahmoune, F. Martin, G.G. Ross, J. Appl. Phys. 105 (2009) 013521.
[5] F. Martin, G.G. Ross, unpublished results.
[6] J.P. Biersack, L.G. Haggmark, Nuclear Instrum. Methods 174 (1980) 257.
[7] G. Faraci, S. Gibilisco, P. Russo, A.R. Pennisi, S. La Rosa, Phys. Rev. B 73 (2006) 033307.
[8] D. Barba, F. Martin, G.G. Ross, Nanotechnology 19 (2008) 115707.
[9] C.P. Herrero, Phys. Stat. Sol. (b) 220 (2000) 857.

[10] M. Cardona, Phys. Stat. Sol. (b) 220 (2000) 5.
[11] F. Widulle, T. Ruf, A. Göbel, I. Silier, E. Schönherr, M. Cardona, J. Camacho, A. Cantarero, W. Kreigseis, V.I. Ozhogin, Phys. B 263–264 (1999) 381.
[12] S. Tsoi, H. Alawadhi, X. Lu, J.W. Ager III, C.Y. Liao, H. Riemann, E.E. Haller, S. Rodriguez, A.K. Ramdas, Phys. Rev. B 70 (2004) 193201.
[13] J. Martin, F. Cichos, F. Huisken, C. Borczyskowski, Nano Lett. 8 (2008) 656.
[14] Y. Sui, X. Huang, Z. Ma, W. Li, F. Qiao, K. Chen, K. Chen, J. Phys. Condens. Matter 15 (2003) 5793.
[15] N. Daldosso, M. Luppi, S. Ossicini, E. Degoli, R. Magri, G. Dalba, P. Fornasini, R. Grisenti, F. Rocca, L. Pavesi, S. Boninelli, F. Priolo, C. Spinella, F. Iacona, Phys. Rev. B 68 (2003) 085327.
[16] Y.Q. Wang, R. Smirani, G.G. Ross, J. Crystal Growth 294 (2006) 486.